INSTITUTO DE FÍSICA

preprint

IFUSP/P-250

A MODIFIED VERSION OF THE MONTE CARLO COMPUTER CODE FOR CALCULATING NEUTRON DETECTION EFFICIENCIES

by

K. Nakayama and E.F. Pessoa
Instituto de Física, Universidade de São Paulo

and

R.A. Douglas
Instituto de Física Gleb Wataghin
Universidade Estadual de Campinas

UNIVERSIDADE DE SÃO PAULO
INSTITUTO DE FÍSICA
Caixa Postal - 20.516
Cidade Universitária
São Paulo - BRASIL

A MODIFIED VERSION OF THE MONTE CARLO COMPUTER CODE FOR CALCULATING NEUTRON DETECTION EFFICIENCIES

Kanzo Nakayama and Elizabeth Farrelly Pessoa

Laboratório do Acelerador Pelletron
Instituto de Física, Universidade de São Paulo
São Paulo, Brasil.

and

Ross Alan Douglas

Instituto de Física Gleb Wataghin
Universidade Estadual de Campinas
São Paulo, Brasil.

ABSTRACT

A calculation of neutron detection efficiencies has been performed for organic scintillators using the Monte Carlo Method. Effects which contribute to the detection efficiency have been incorporated in the calculations as thoroughly as possible. The reliability of the results is verified by comparison with the efficiency measurements available in the literature for neutrons in the energy range between 1 and 170 MeV with neutron detection thresholds between 0.1 and 22.0 MeVee.

December/1980

1. INTRODUCTION

A good deal of effort has been devoted to the calculation of neutron detection efficiencies of organic scintillators for a wide range of neutron energies (1 to 200 MeV) using the Monte Carlo method[1-4]. The results are often in disagreement with one another and are unable to reproduce the experimentally determined values of the neutron detection efficiencies. The principal cause of these discrepancies is due to the scarcity, at the time, of accurate values of the many parameters necessary for the calculations. For this reason these calculations were limited to very special cases so that even when they were able to reproduce experimental results, ample doubt remained as to their reliability in more extensive applications.

More recently, several articles have appeared in the literature[5,6] where the Monte Carlo method was used with a great deal of success to reproduce the existing values of experimental neutron detection efficiencies. However, these calculations do present certain systematic discrepancies stemming from the omission of a few of the factors which contribute to the detection process and from somewhat precarious estimations of some of the quantities which enter the calculations.

The purpose of this work was to improve the reliability and accuracy of the calculations of neutron detection efficiencies by including, as much as possible, the many effects involved in the detection process and by reevaluating the parameters more carefully. The criterion for acceptance of the new values is their ability to reproduce the experimental results of the efficiency measurements and so it should be emphasized that our accuracy in calculating the efficiencies is limited by the precision of the efficiency measurements themselves ($\sim$ 5%). The calculations have been extended to a neutron energy range from

1 to 170 MeV with detection thresholds between 0.1 and 22.0 MeVee.

Section 2 is a discussion of our particular version of the Monte Carlo calculation and the corresponding modified computer code which is used. Section 3 is a presentation of the results and a comparison with the experimental values of neutron detection efficiencies available in the literature for a variety of cases. Section 4 contains the conclusions.

2. THE MONTE CARLO CALCULATION

The structure of the Monte Carlo computer code is basically that developed by Devos et al[4]. Our version, however, extends the calculations from the original maximum neutron kinetic energy of 15 MeV up to 200 MeV. To do this carefully, various modifications were necessary, the most important being summarized as follows:

A. Inclusion of the channels $^{12}C(n,np)^{11}B$ and $^{12}C(n,2n)^{11}C$ in the interaction process of the neutrons with the scintillator and employment of improved values of the neutron induced cross sections and their kinematics.

B. Utilization of more adequate expressions to represent the light production response of the scintillator.

C. Inclusion of the light attenuation effects.

D. Consideration of the effect of finite resolution on the amplitudes of the light pulses.

E. Employment of better 'range-energy' relations for the charged particles involved in the interaction processes.

F. The use of relativistic kinematics.

We will briefly discuss these items and their importance.

A. Improvement of the Cross Sections.

Del Guerra[5] has reported an extensive compilation of the total cross section measurements available for various n-C processes and the n-p scattering process along with an excellent discussion of their relative importance for neutron detection in organic scintillators. McNaughton et al[3] in addition to a similar discussion also emphasized the importance of the $^{12}C(n,np)^{11}B$ reaction, above 20 MeV neutron energy. Thus the totality of processes assumed to contribute to the detection efficiency are the elastic scattering of neutrons by ^{12}C and by protons and the following five inelastic scattering processes:

1. $^{12}C(n,n'\gamma)^{12}C^*$ (Q = -4.43 MeV)
2. $^{12}C(n,\alpha)^{9}Be$ (Q = -5.709 MeV)
3. $^{12}C(n,n')3\alpha$ (Q = -7.281 MeV)
4. $^{12}C(n,np)^{11}B$ (Q = -15.69 MeV)
5. $^{12}C(n,2n)^{11}C$ (Q = -20.30 MeV)

Cross section data for both elastic scattering processes and the first three inelastic processes were essentially obtained from Del Guerra[5]. In the case of the channel $^{12}C(n,np)$ we used not only those experimental values given by Del Guerra[5], but also the cross section value at 56 MeV reported by McNaughton et al[3]. It should be mentioned here that the McNaughton cross section at 56 MeV also includes all final states in which a free proton occurs (e.g. $^{12}C(n,2p)$). However, since the $^{12}C(n,np)^{11}B$ channel predominates (about 90% according to Kellogg's data[7]) for clarity we refer to all the processes as merely the $^{12}C(n,np)$ channel.

The $^{12}C(n,2n)$ cross sections were obtained from G. Bathow et al[8] and J.R. Stehn et al[9]. Although this channel

is only 10% of the $^{12}C(n,np)$ cross section, it is sufficient to influence the neutron detection efficiency for large scintillators and for this reason was included in the program

The cross section data for the last two inelastic channels cited above (4,5) also contain large gaps which obliged us to interpolate. The criteria for choosing acceptable cross sections in the interpolated region were i) to connect the regions of experimental values by the smoothest possible curve in the interpolated region, ii) the sum of all separate inelastic channel cross sections considered (five channels) is in agreement with the available experimental non-elastic cross section[5] and iii) at the same time obtain the best agreement between the calculated and measured values of the neutron detection efficiencies.

The angular distributions for the $H(n,n)H$, $^{12}C(n,n)^{12}C$, $^{12}C(n,\alpha)^{9}Be$ and $^{12}C(n,n')3\alpha$ reactions were obtained from the work of Stanton[2].

For the $^{12}C(n,n'\gamma)^{12}C$ processes, the angular distribution of the neutrons was obtained from the data of Glasgow et al[10] and was assumed to be independent of energy. The calculational form used was

$$\frac{d\sigma_{nn'}}{d\Omega} = \sum_{L=0}^{4} a_L P_L(\cos\theta^*) \qquad \theta^* = \text{C.M. angle}$$

with

$$a_o = 27.8 \quad a_1 = 16.9 \quad a_2 = 34.8 \quad a_3 = 7.3 \quad a_4 = 6.4 \quad \text{in mb/sr.}$$

The angular distribution of the gamma rays emitted has a complicated dependence on energy[11] which was ignored completely

and substituted by an average value represented by the formula

$$\frac{d\sigma_{n\gamma}}{d\Omega} = (1.03 - 0.09 \cos^2\theta) \frac{mb}{sr} \qquad \theta = \text{lab. angle}$$

It was furthermore assumed that the 4.43 MeV gamma ray involved in the deexcitation of the first excited state of ^{12}C interacts with the scintillator material exclusively by Compton scattering.

The angular distribution of the proton from the reaction $^{12}C(n,np)$ was taken from the data of McNaughton et al[3] at 56 MeV and considered independent of energy. The kinematics for this reaction were also obtained from McNaughton et al[3]. It was also assumed that the angular distribution of the neutron was the same as that of the proton.

After accounting for the effect of the different Q values on the kinematics, the angular distribution for the $^{12}C(n,2n)$ reaction was assumed to be the same as the $^{12}C(n,np)$ reaction. Recently, Cecil et al[6] has published a treatment of these two reaction channels which is in essence the same as in this work.

The kinematics of the $^{12}C(n,n')3\alpha$ reaction were kept the same as those used by Stanton[2].

B. The Scintillator Response Function.

The quantity of light produced in an organic scintillator may be expressed in terms of equivalent electron energy (MeVee). The equivalent electron energy T_e, to which the heavier charged particles correspond, are obtained for energies above 1 MeVee, from the following expression parametrized by Madey et al[12] for the scintillators NE102, NE228 and NE224 and by Cecil et al[6] for the scintillator NE213 by adjustment to the experimental data

$$T_e = a_1 T_p - a_2(1 - \exp(-a_3 T_p^{a_4})) \qquad (2.1)$$

T_e and T_p are expressed in MeV and the values recommended for the coefficients are given in Table 1a for the different scintillator materials.

For energies below 1 MeVee, the equivalent electron energies are obtained using the formula

$$T_e = b_1 T_p + b_2 T_p^2 \qquad (2.2)$$

where T_e and T_p are expressed in MeV and the coefficients obtained from the work of Bachelor et al[13], normalized to those of equation (2.1) at 1 MeVee, are given in Table 1b. For heavy ions we have used the equation (2.2) in all the range of energy.

C. The Effect of the Light Attenuation.

The importance of the light attenuation by the scintillator itself increases with size. Exact calculation of the efficiency of light collection in a scintillator is extremely difficult. However, Clark[14] derived an appropriate relation which has been widely used[14-16] especially for scintillators whose transverse dimensions are larger than the longitudinal dimension. We have applied this formula to the alternative case (transverse dimensions much smaller than the longitudinal dimension) and found that the formula of Clark[14] underestimates the collection efficiency. To correct for this we derived the approximation.

$$\epsilon = \beta(st_o + (1-s)\, t_1 r) \qquad (2.3)$$

where,

ϵ is the light collection efficiency.

β is an optical coupling constant for the scintillator-photo-tube interface.

s is the total solid angle subtended by the photomultiplier with reference to the point in the scintillator at which the light is produced.

t_o is equal to $\exp(-al_o)$, where a is the linear coefficient of light absorption in the scintillator and l_o is the average distance travelled by the light from its point of emission within the solid angle s, to the photocathode.

r is the reflection coefficient at the scintillator walls.

t_1 is equal to $\exp(-al_1)$, where l_1 is the average distance between those light emission points which lie outside the solid angle s and the photocathode.

Typical values of r and a are given in Table 2. A value of $\beta = 1$ was assumed in all cases. In addition it was simply supposed that $l_o = d_i$ and $l_1 = 2L - d_i$ where L is the scintillator total length and d_i is the distance between the photocathode and the ith point at which the light is emitted.

The value of the detection threshold (in terms of electron energy) is usually obtained experimentally using well known gamma sources. Let us suppose that the gamma rays have an energy E_γ and the discrimination level is adjusted for these gammas. However, since only a part of the light generated by the electrons which the gamma scattering process produces in the scintillator actually reaches the photocathode, the effective value of the detection threshold would be $(1 - F^\gamma)E_\gamma$ where

$$F^\gamma = \frac{\sum_{ij} (1 - \epsilon_{ij}^\gamma) L_{ij}}{\sum_{ij} L_{ij}}$$

The labels i,j denote the ith interaction of the jth incident gamma ray, the quantity L_{ij} represents the amount of light produced by the electron which was generated and ϵ^{γ}_{ij} is the light collection efficiency of formula (2.3).

D. The Amplitude Resolution.

The registration of an event in the scintillator produces an electric pulse at the plate of the photomultiplier whose distribution in amplitude (resolution) is reasonably well represented by a Gaussian function[17] whose width varies as $(\bar{v})^{1/2}$ where $\bar{v}$ is the average value of the amplitude of the pulse produced by monoenergetic ionizing particles.

In order to simulate this effect of finite resolution, we employed the same formula as Stanton[2] parametrized in terms of the minimum average energy necessary to produce a photoelectron at the photocathode, P_o. The mean square deviation is given as

$$\sigma_p = P_o\left(\frac{P}{P_o} + 0.5\right)^{1/2} \qquad (2.4)$$

where P is the quantity of light impinging on the photocathode. A value of $P_o = 10^{-3}$ MeVee was chosen in accordance with the suggestions of De Leo et al[16] in his detailed work which justified the applicability of equation (2.4). This value was maintained for all the photomultiplier tubes.

E. The Range Energy Relation for the Charged Particles.

The need for accurate range energy relations is critical in the case of electrons and photons in order to determine the fraction of total energy imparted to the scintillator. Watson and Graves[18] discuss the importance of this

effect.

Empirical relations are used in all cases. For protons we used the following relation given by Cecil et al[6] whose coefficients are evaluated by fitting to the experimental data for the scintillator Pilot B

$$\ell_n(R_p) = \sum_{n=0}^{5} a_n \, (\ell_n \, T_p)^n$$

$$T_p > 0.5 \text{ MeV} \qquad (2.5)$$

$$\ell_n(T_p) = \sum_{n=0}^{5} b_n \, (\ell_n \, R_p)^n$$

Values of the coefficients a_n and b_n are presented in Table 3. The range R_p is expressed in mm and the proton energy T_p in MeV .

For the cases where $T_p < 0.5$ MeV we used the formula given by Watson and Graves[18] for the NE102 plastic scintillator

$$R_p = 0.0029 \, T_p^{1.667} \quad \text{cm}$$

$$T_p = \frac{1}{0.0029} \, R_p^{0.6} \quad \text{MeV} \qquad (2.6)$$

These equations, (2.5) and (2.6), are generally used for any scintillator whose chemical composition and density is similar to NE102 or Pilot B.

For the liquid scintillator NE213 we used the relation

$$R_p = f(T_p)$$

with

$$f(T_p) = \begin{cases} 0.00315\ T_p^{1.724} & T_p > 10 \text{ MeV} \\ 0.00315\ T_p^{1.667} & 10 \text{ MeV} > T_p > 3 \text{ MeV} \\ 0.0029\ T_p^{1.667} & 3 \text{ MeV} > T_p \end{cases}$$

where

$$T_p = f^{-1}(R_p)$$

These expressions were derived by obtaining fits to the data of Craun[19] to within 1% for $T_p > 3$ MeV.

For alpha particles we used the relations

$$R_\alpha = f(T_p/4)$$

$$T_\alpha = 4\ f^{-1}(R_\alpha)$$

For electrons we used an expression given by Evans[20]

$$R_e = d(0.52\ T_e - 0.09) \quad \text{cm}$$

$$T_e = (1.92\ d\ R_e - 0.17) \text{ MeV}$$

where d is the density of the detector material in g/cm^3.

F. Relativistic Kinematics.

For extension of the calculations up to 200 MeV incident neutrons, it was deemed necessary to modify the original program of Devos et el[4] to furnish relativistic kinematics in all the reaction channels.

3. COMPARISON OF THE CALCULATED NEUTRON EFFICIENCIES AND THE EXPERIMENTAL VALUES

Many measurements of neutron detection efficiencies exist in the literature. A particular set of measurements determines the efficiencies for a certain scintillator material of specified dimensions, in a given range of incident neutron energies, at various detection thresholds. For each data set, we have applied our Monte Carlo computer code with input information appropriate to the experimental conditions. The calculated detection efficiencies were then compared to the measurements. A compilation of the results will now be made.

Figure 3.1 shows a group of results for the plastic scintillators NE102 and NE102A with longitudinal dimensions between 5.08 cm and 15.2 cm. Figures 3.1a and 3.1b compare the calculations to the data of Hunt et al[21] for the NE102 plastic scintillator (ϕ = 10.27 cm , L = 5.08 cm) for incident neutron energies up to 40 MeV and three different neutron detection thresholds 0.96 , 2.40 and 1.07 MeVee. As can be seen, the agreement is excellent even for neutron energies near the detection threshold. Figure 3.1c is a comparison of the calculations with the data of McNaughton et al[22] for the NE102A plastic scintillator (ϕ = 7.10 cm , L = 15.20 cm) for neutron energies up to 40 MeV and for two different thresholds, 1.0 and 4.2 MeVee. It is seen that the 4.2 MeVee case shows some discrepancy (~10%) in the neutron energy range between 16 and 22 MeV. Figure 3-1d shows our results for the data of Riddle et al[23] also obtained for the NE102 plastic scintillators (ϕ = 17.73 cm , L = 7.60 cm). Good agreement is obtained between the calculated curves and the experimental points in the region where they are available.

Figure 3.2 shows results for the same class of

scintillator as in Figure 3-1 but with much larger longitudinal dimensions. Figure 3-2a shows an excellent fit of the Monte Carlo calculated efficiencies to the data of Crabb et al[24] for the NE102A scintillator (ϕ = 30.50 cm , L = 28.60 cm) for incident neutron energies up to 120 MeV and a threshold of 2.5 MeVee. Figure 3-2b compares our calculations with the data of Young et al[25] for NE102 (ϕ = 12.70 cm, L = 30.50 cm) for neutron energies up to about 160 MeV and detection thresholds of 2.0 4.0 and 16.0 MeVee. A small discrepancy of the order of 10% or less appears in the neutron energy range between 100 and 170 MeV for those experimental points referring to the 2.0 MeVee threshold.

Figure 3-3 shows our results for a group of liquid scintillators. Figure 3-3a shows the fits we obtained to the data of Hunt et al[21] for the liquid scintillator NE228 (ϕ = = 10.27 cm, L = 5.08cm) for neutrons up to 40 MeV and a detection threshold of 0.57 MeVee. Figure 3-3b is a comparison of the calculation with the data of Drosg[26] for the liquid scintillator NE213 (ϕ = 12.00 cm, L = 5.60 cm) for neutron energies up to about 25 MeV and detection thresholds of 0.254 , 1.02 and 2.54 MeVee. In particular, the reproduction of the details of the structure present in these precise measurements is in general quite good. Figure 3-3c shows the calculation applied to the case of the extremely low neutron detection threshold of 0.05 MeVee used to obtain the data of Thornton et al[27] for the liquid NE213 scintillator (ϕ = 10.20 cm, L = 1.83 cm).

Figure 3-4 is a comparison of the calculations with the measured efficiencies of Parsons et al[28] for a very thick NE224 liquid scintillator (ϕ = 7.00 cm, L = 45.00 cm) for neutron energies up to 340 MeV with a detection threshold of 1.3 MeVee. The fit is in general quite reasonable, the maximum discrepancies being of the order of 11%.

Figure 3.5 shows the neutron efficiency measurements of Crabb et al[24] for two different incident neutron energies 40 and 120 MeV and for various geometries of the incident neutron beam. The Monte Carlo calculations are in excellent agreement indicating that the treatment of scintillator edge effects is correct.

Figure 3-6 illustrates the effect on the efficiency of the shape of the proton and neutron angular distributions for the channel $^{12}C(n,np)^{11}B$ above 20 MeV incident neutron energy. The experimental points are those of McNaughton (see Fig. 3-1c). The dashed curve is calculated assuming that the proton and neutron angular distributions are both isotropic in the Center of Mass system. The full curve was obtained by supposing that the angular distributions of the proton and neutron possess a $\cos^2\theta$ angular dependence in the Laboratory system. The results show that the latter supposition is the better one with the consequence that the detector efficiency is enhanced for very long scintillators.

Figure 3-7 illustrates the importance of accounting for the light attenuation occuring in the scintillator itself and the influence this attenuation has on the determination of the true neutron detection threshold. The experimental points for comparison are the data of Drosg (see Fig. 4-3a). The dashed curves are the result of the Monte Carlo calculations when the light attenuation is omitted and the full curves are the results obtained when it is included. The sensitivity of this effect on neutron energies near threshold is quite large as expected.

4. CONCLUSIONS

Calculations of neutron detection efficiencies for

the commonly available organic scintillators were carried out using a modified Monte Carlo method. The results agree well with the experimental measurements of efficiencies which exist in the literature. We are able to conclude that in general the calculated values of the efficiencies are reliable to within 5% in the neutron energy range of 1 to 170 MeV with detection thresholds between 0.1 and 22.0 MeVee.

It is interesting to compare our results with those of Del Guerra and Cecil. For the most part they are quite similar, although our results seem to fit the experimental efficiencies of McNaughton and especially those of Hunt somewhat better than the Del Guerra results. These differences are essentially due to the improved treatment of the $^{12}C(n,np)^{11}B$ channel. In the region of neutron energies near the detection threshold, our results agree more closely with the experimental data than Cecil's results. We believe that these differences are due to the inclusion of light attenuation corrections.

ACKNOWLEDGEMENTS

We would like to acknowledge the assistance of Dr. Ross Barnett, Dr. Michael W. McNaughton and Dr. Richard Madey who sent us copies of programs. One of us (K.N.) received a schoolarship from the São Paulo Foundation for the Advancement of Science (FAPESP) and the project was financed through grants from the Brazilian National Research Council (CNPq) and the Brazilian Foundation for the Support of Research Projects (FINEP).

TABLE 1a

Coefficients in the light response function, eq.(2.1), for protons and alphas in various scintillators. Energy of particles greater than 1.0 MeVee.

Particle and scintillators	Coefficients			
	a_1	a_2	a_3	a_4
p , NE-102	0.95	8.0	-0.1	0.90
p , NE-213	0.83	2.82	0.25	0.93
p , NE-224	1.0	8.2	0.1	0.88
p , NE-228 and NE-228A	0.95	8.4	0.1	0.90
α , all scintillators	0.41	5.9	0.065	1.01

TABLE 1b

Coefficients in the light response function, eq.(2.2), for protons, alphas and heavy ions in various scintillators. Energy of protons and alphas up to 1.0 MeVee. For heavy ions, it is valid for all the range of energies.

Particle and scintillators	Coefficients	
	b_1	b_2
p , NE-102	0.196	0.026
p , NE-213	0.215	0.028
p , NE-224	0.228	0.030
p , NE-228 and NE-228A	0.166	0.022
α , all scintillators	0.046	0.007
heavy ions, all scintillators	0.017	0

TABLE 2

Typical values of the reflection coefficient r and linear coefficient of light absorption a .

Scintillator	Coefficients	
	r	a (cm^{-1})
NE-213	0.96 a)	$\frac{1}{200}$ b,c)
NE-102	0.96	$\frac{1}{170}$ b)

a) from the reference (30)
b) from the reference (29)
c) from the reference (31)

TABLE 3

Coefficients in the range energy relation, eq.(2.5), for protons in the scintillator Pilot B.

	n=0	n=1	n=2	n=3	n=4	n=5
a_n	-3.8103	1.617	8.193×10^{-2}	-2.0364×10^{-2}	3.147×10^{-3}	-2.321×10^{-4}
b_n	2.1964	0.56148	1.0055×10^{-3}	8.885×10^{-5}	1.821×10^{-4}	2.742×10^{-5}

FIGURE CAPTIONS

FIG. 3-1 - Comparison of efficiency measurements with the Monte Carlo predictions for plastic scintillators between 5.08 and 15.2 cm thick.

FIG. 3-2 - Comparison of efficiency measurements with the Monte Carlo prediction for plastic scintillators 28.60 and 30.50 cm thick.

FIG. 3-3 - Comparison of efficiency measurements with the Monte Carlo prediction for liquid scintillators between 1.83 and 5.6 cm thick.

FIG. 3-4 - Comparison of efficienty measurements with the Monte Carlo prediction for liquid scintillator 45.0 cm thick.

FIG. 3-5 - Detection efficiency vs radial position for 40 and 120 MeV neutron energy. The contribution outside the scintillator limits is due to the container. The horizontal error-bars indicate the beam width. The full lines are the Monte Carlo predictions.

FIG. 3-6 - The effect on the efficiency of the shape of the proton and neutron angular distributions for the channel $^{12}C(n,np)^{11}B$. The dashed curve is calculated assuming that the proton and neutron angular distributions are both isotropic in the Center of Mass while the full curve corresponds to the forward peaked angular distribution.

FIG. 3-7 - The effect of the light attenuation in the scintillator. The full and dashed curves correspond respectively to the calculations with and without the light attenuation.

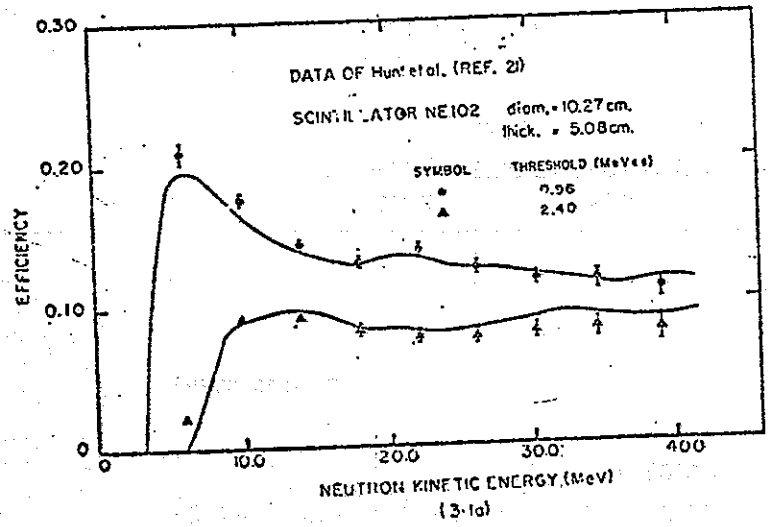

(3-1a)

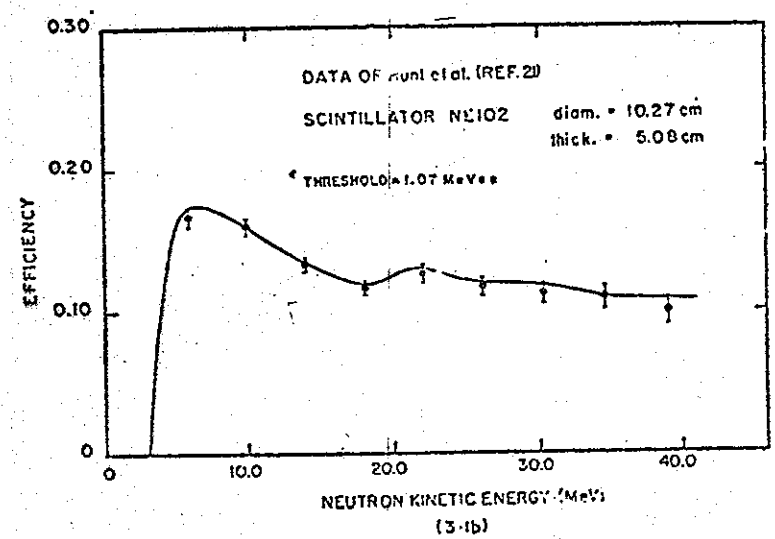

(3-1b)

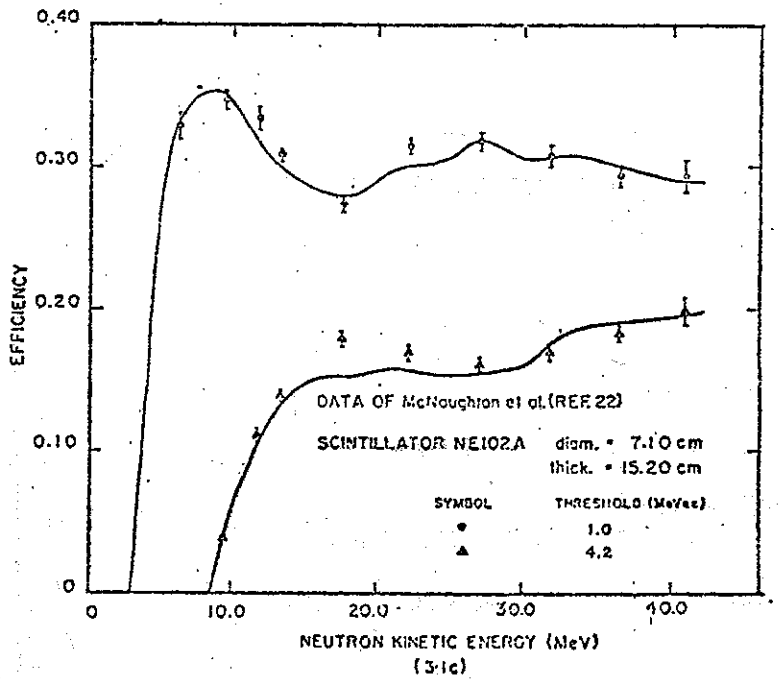

(3-1c)

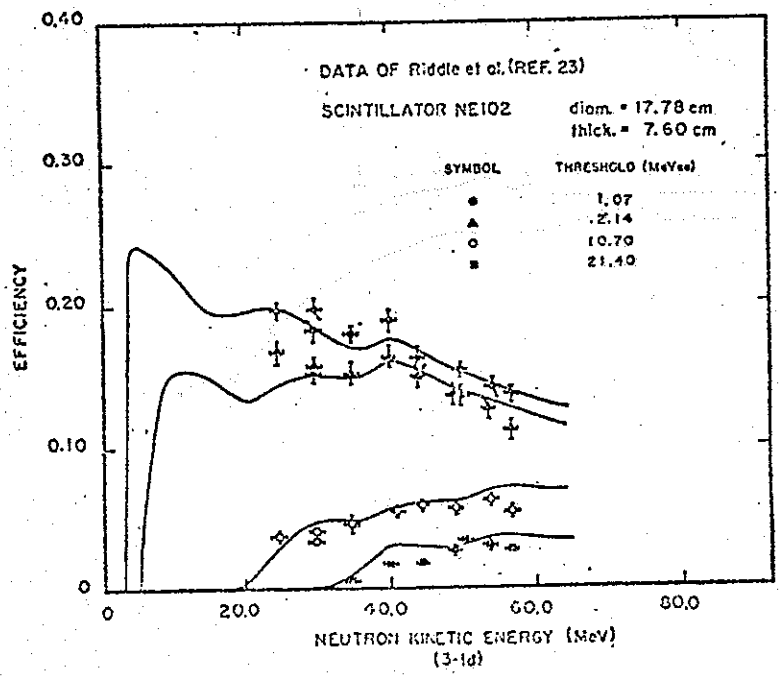

(3-1d)

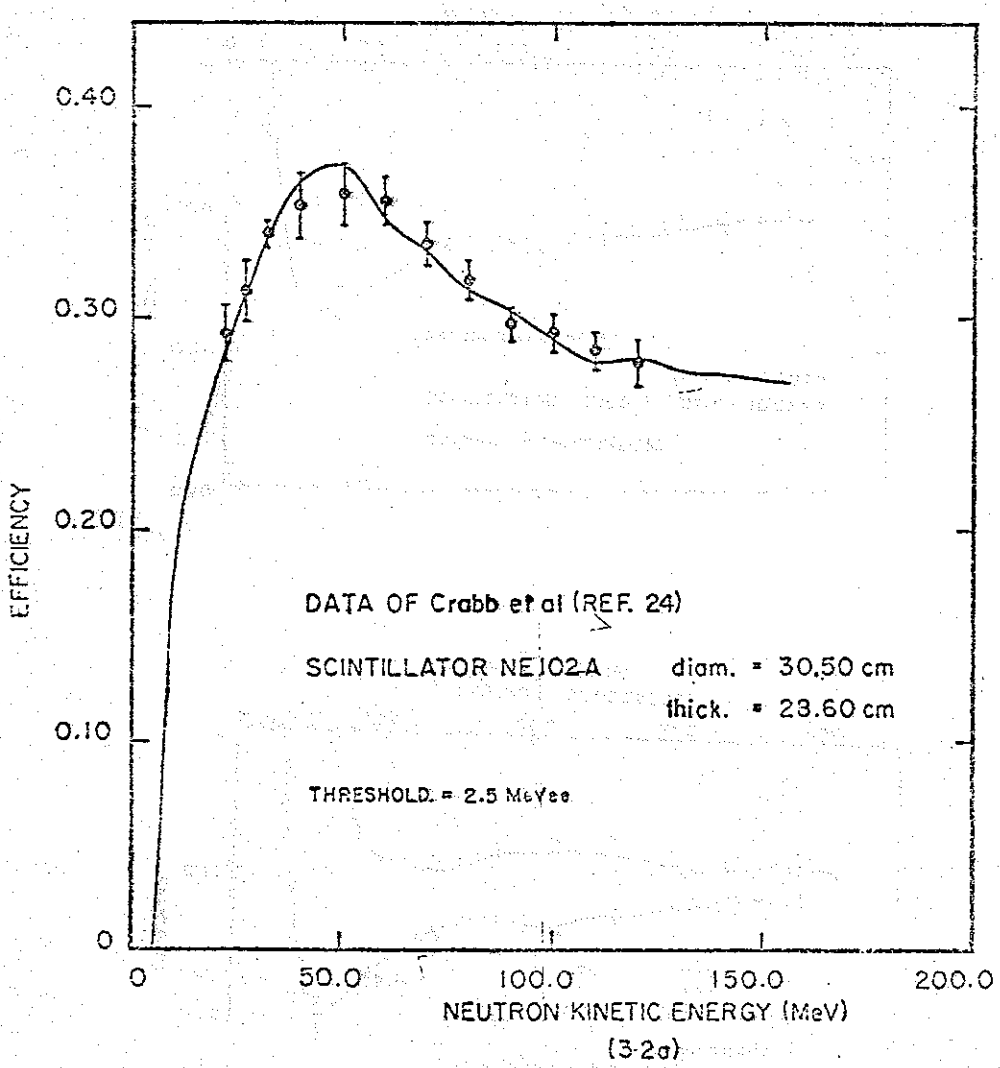
0.40
0.30
0.20
0.10
0
EFFICIENCY
DATA OF Crabb et al (REF. 24)
SCINTILLATOR NE102-A
diam. = 30.50 cm
thick. = 23.60 cm
THRESHOLD. = 2.5 MeVee
0
50.0
100.0
150.0
200.0
NEUTRON KINETIC ENERGY (MeV)

(3-2a)

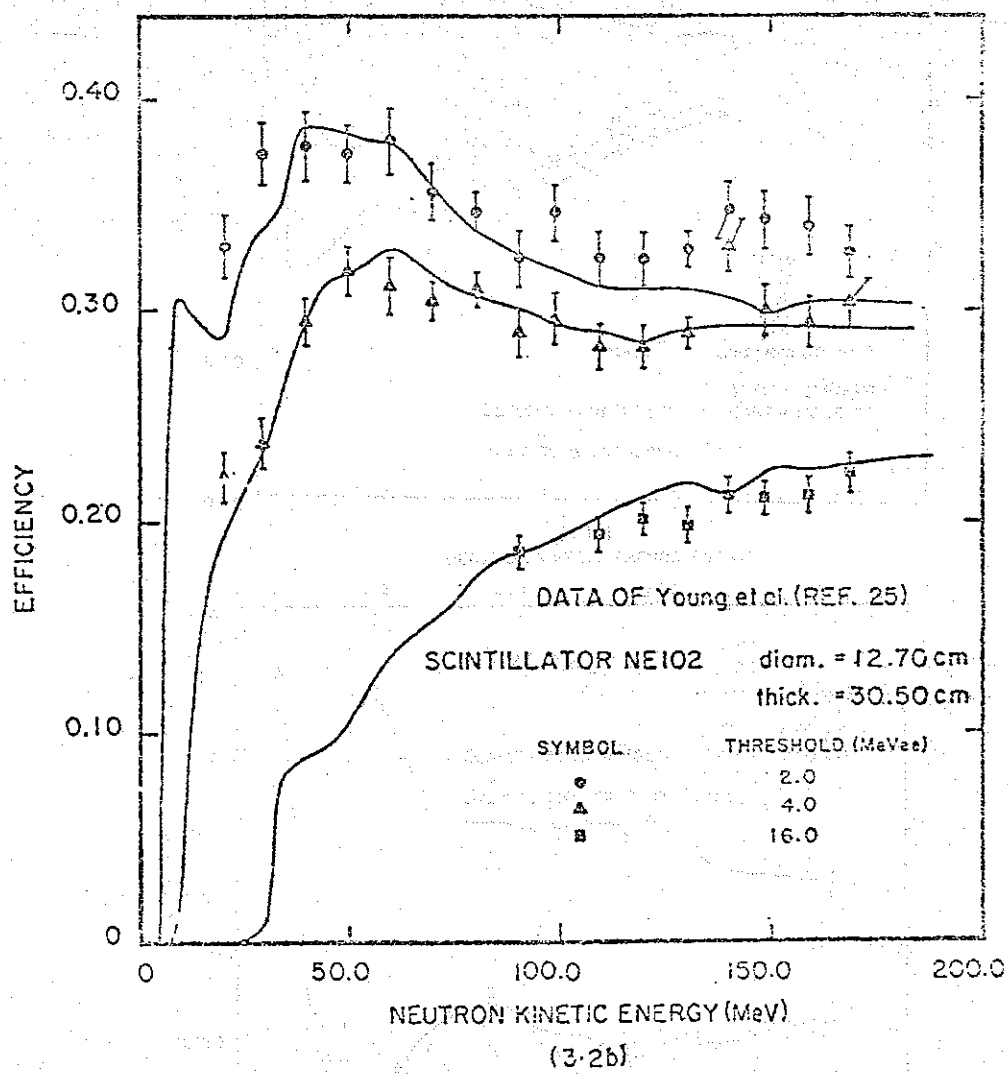
0.40
0.30
0.20
0.10
0
EFFICIENCY
DATA OF Young et al. (REF. 25)
SCINTILLATOR NE102
diam. = 12.70 cm
thick. = 30.50 cm
SYMBOL
THRESHOLD (MeVee)
2.0
4.0
16.0
0
50.0
100.0
150.0
200.0
NEUTRON KINETIC ENERGY (MeV)

(3-2b)

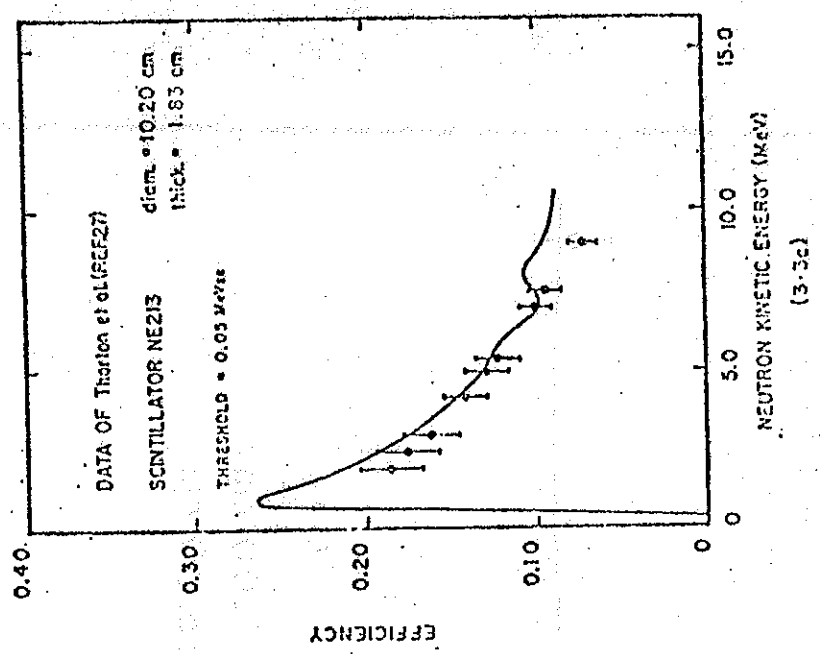
DATA OF Thorton et al.(REF.27)
SCINTILLATOR NE213
diam. = 10.20 cm
thick. = 1.83 cm
THRESHOLD = 0.05 MeVee
EFFICIENCY
0.40
0.30
0.20
0.10
0
0
5.0
10.0
15.0
NEUTRON KINETIC ENERGY (MeV)

(3-3a)

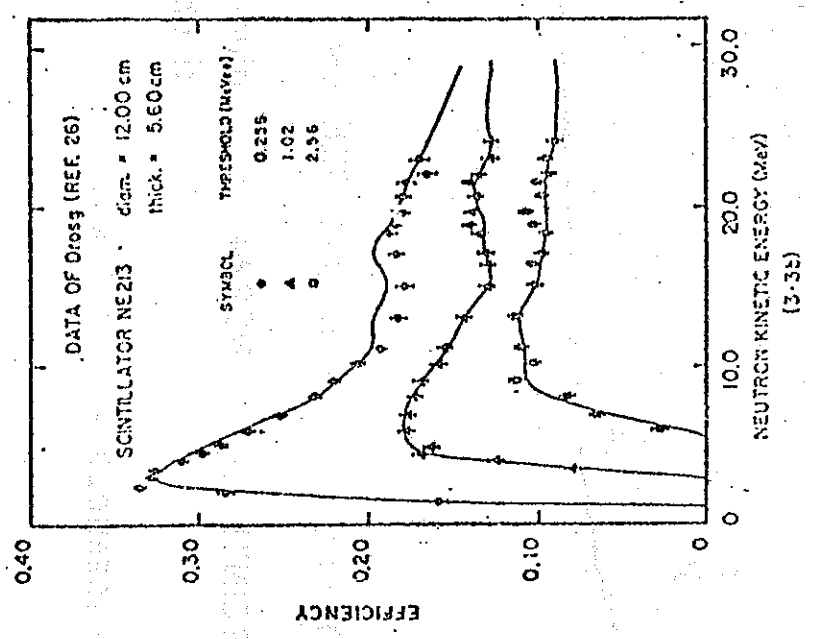
DATA OF Drosg (REF. 26)
SCINTILLATOR NE213
diam. = 12.00 cm
thick. = 5.60 cm
SYMBOL
THRESHOLD (MeVee)
0.235
1.02
2.56
EFFICIENCY
0.40
0.30
0.20
0.10
0
0
10.0
20.0
30.0
NEUTRON KINETIC ENERGY (MeV)

(3-3b)

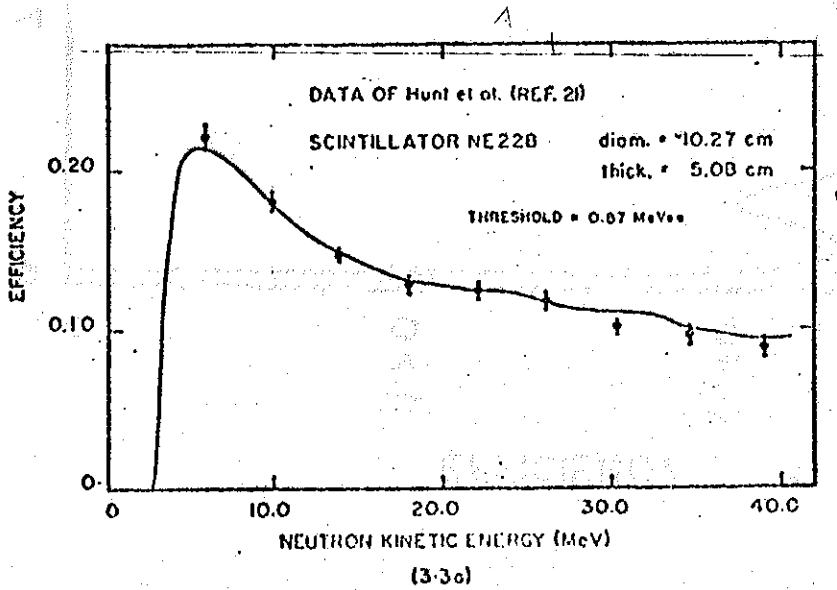
DATA OF Hunt et al. (REF. 28)
SCINTILLATOR NE228
diam. = 10.27 cm
thick. = 5.08 cm
THRESHOLD = 0.07 MeVee
EFFICIENCY
0.20
0.10
0
0
10.0
20.0
30.0
40.0
NEUTRON KINETIC ENERGY (MeV)

(3-3c)

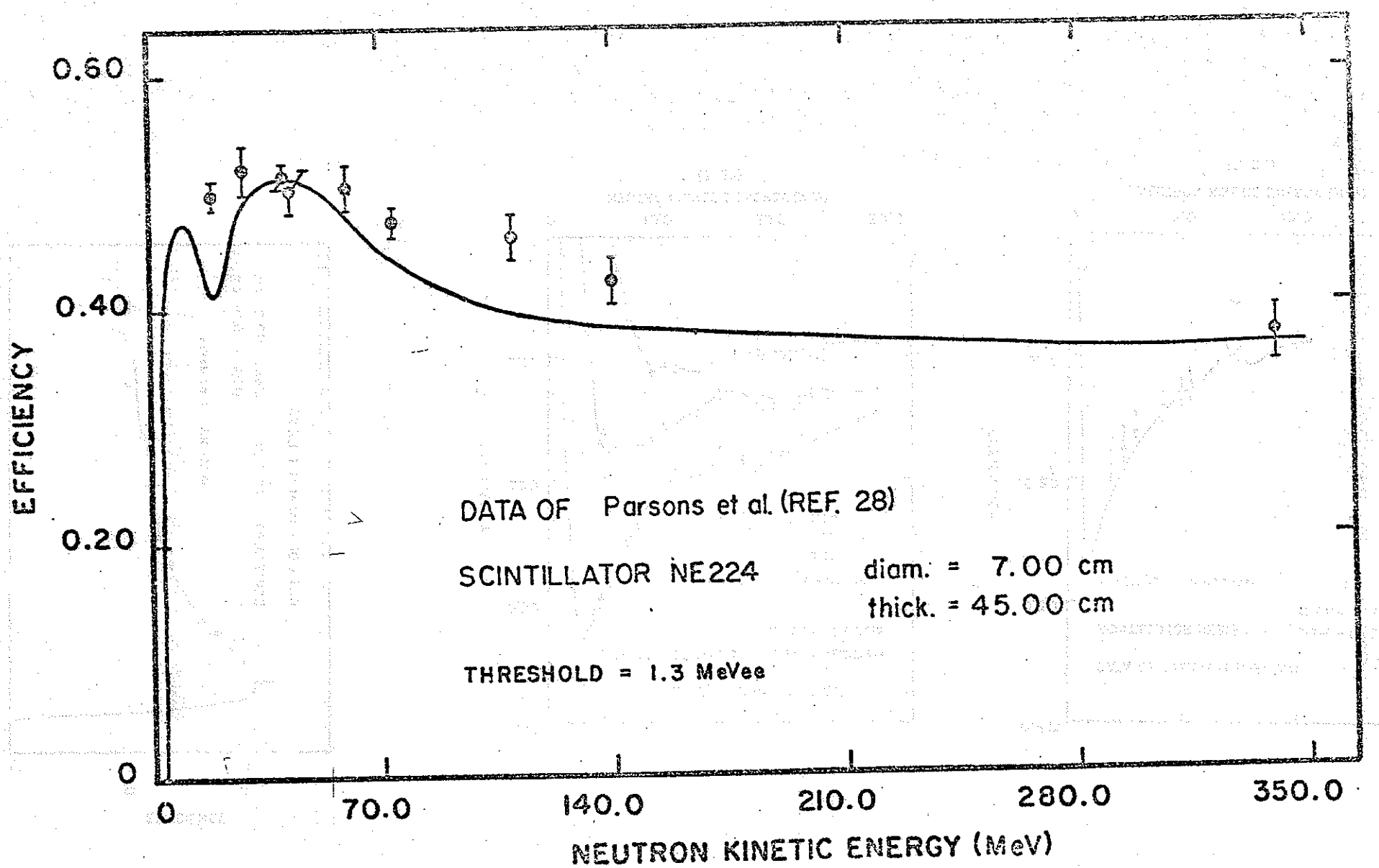
0.60
0.40
0.20
0
EFFICIENCY
DATA OF Parsons et al. (REF. 28)
SCINTILLATOR NE224
diam. = 7.00 cm
thick. = 45.00 cm
THRESHOLD = 1.3 MeVee
0
70.0
140.0
210.0
280.0
350.0
NEUTRON KINETIC ENERGY (MeV)

(3·4)

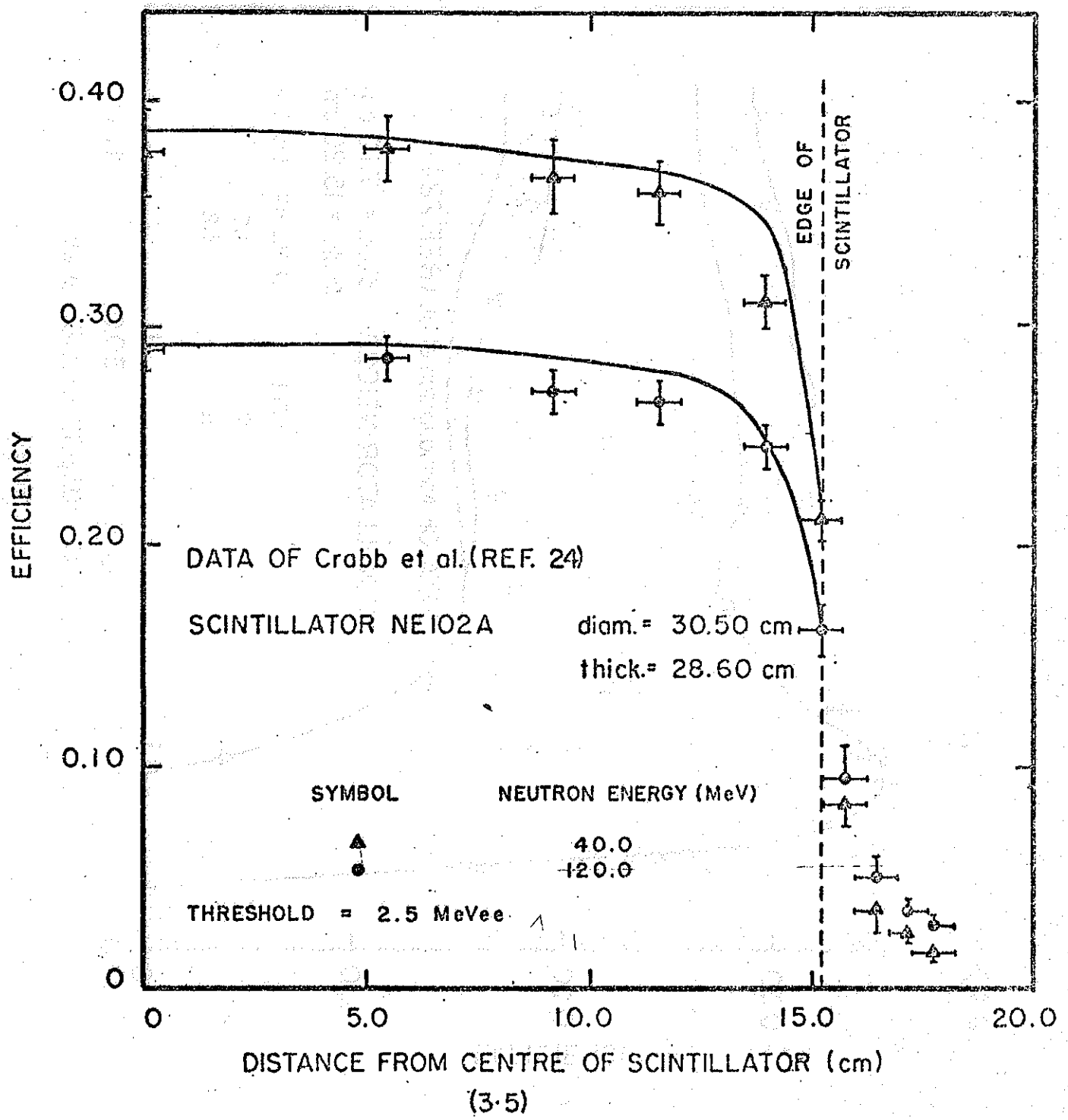
0.40
0.30
0.20
0.10
0
EFFICIENCY
EDGE OF SCINTILLATOR
DATA OF Crabb et al. (REF. 24)
SCINTILLATOR NE102A
diam. = 30.50 cm
thick. = 28.60 cm
SYMBOL
NEUTRON ENERGY (MeV)
40.0
120.0
THRESHOLD = 2.5 MeVee
0
5.0
10.0
15.0
20.0
DISTANCE FROM CENTRE OF SCINTILLATOR (cm)

(3·5)

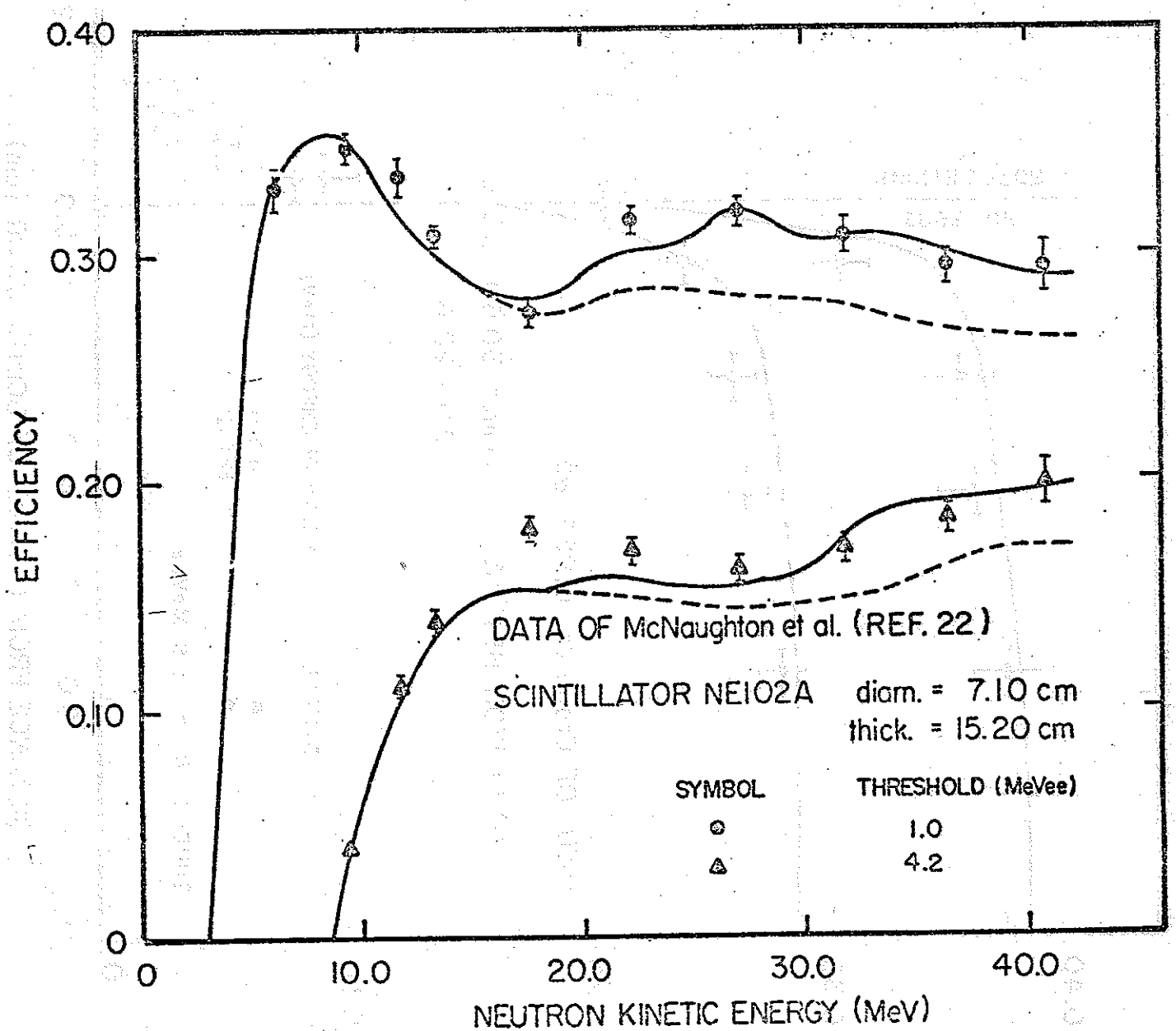
0.40
0.30
0.20
0.10
0
EFFICIENCY
0
10.0
20.0
30.0
40.0
NEUTRON KINETIC ENERGY (MeV)
DATA OF McNaughton et al. (REF. 22)
SCINTILLATOR NE102A
diam. = 7.10 cm
thick. = 15.20 cm
SYMBOL
THRESHOLD (MeVee)
1.0
4.2

(3·6)

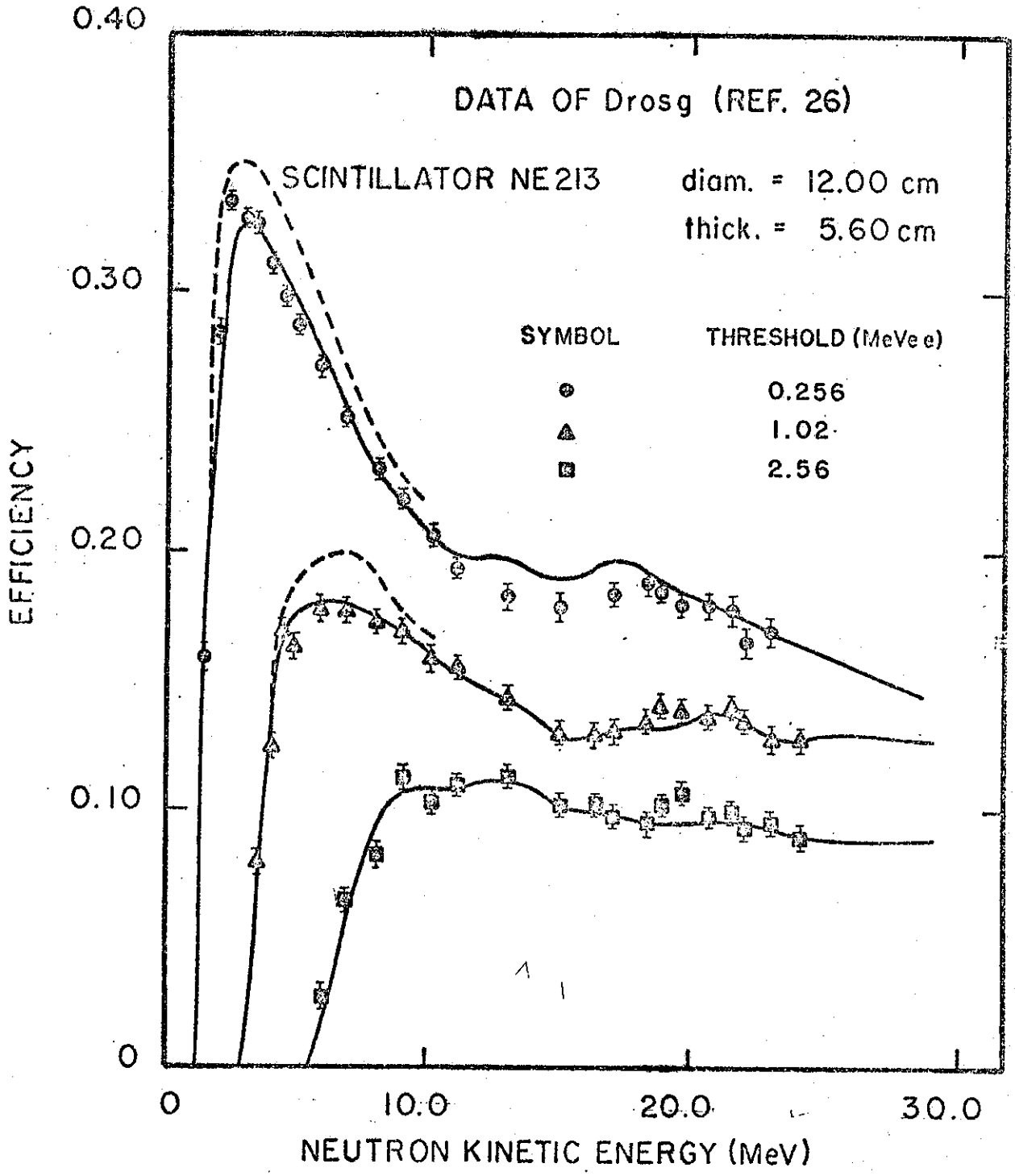
DATA OF Drosg (REF. 26)
SCINTILLATOR NE213
diam. = 12.00 cm
thick. = 5.60 cm
SYMBOL
THRESHOLD (MeVee)
0.256
1.02
2.56
EFFICIENCY
0.40
0.30
0.20
0.10
0
0
10.0
20.0
30.0
NEUTRON KINETIC ENERGY (MeV)

(3·7)

REFERENCES

1. R.E. Textor et al., Oak Ridge National Laboratories, ORNI-4160 (1968).
2. N.R. Stanton, Ohio State University, COO-1545-92 (1971).
3. M.W. McNaughton et al., Nucl. Instr. and Meths. 129 (1975) 241.
4. J. Devos et al., Nucl. Instr. and Meths. 135 (1976) 395.
5. A. Del Guerra, Nucl. Instr. and Meths. 135 (1976) 337.
6. R.A. Cecil et al., Nucl. Instr. and Meths. 161 (1979) 439.
7. D.A. Kellogg, Phys. Rev. 90 (1953) 224.
8. G. Bathow et al., Nucl. Instr. and Meths. 51 (1967) 56.
9. J.R. Stehn et al., BNL-325, vol. 1, 2nd.ed., Suppl. 2 (May, 1964).
10. D.W. Glasgow et al., Nucl. Sci. and Eng. 61 (1976) 521.
11. S. Bashkin and R.R. Carlson, Phys. Rev. 106 (1957) 261.
12. R. Madey et al., Nucl. Instr. and Meths. 151 (1978) 445.
13. R. Batchelor et al., Nucl Instr. and Meths. 13 (1961) 70.
14. G.W. Clark, IRE Transactions on Nucl. Sci. N.S.7 2-3 (1960) 164.
15. P. Kuijper et al., Nucl. Instr. and Meths. 42 (1966) 56.
16. R. De Leo et al., Nucl. Instr. and Meths. 119 (1974) 559.
17. J.J. Samueli et al., Instrumentation Électronique en Physique Nucléaire (Mesures de Temps et D'Énergie), Ed. Masson & Cia (1968) 34.
18. J.W. Watson and R.G. Graves, Nucl. Instr. and Meths. 117 (1974) 541.
19. R.L. Craun and D.L. Smith, Nucl. Instr. and Meths. 80 (1970) 239.
20. R.D. Evans, The Atomic Nucleus, McGraw-Hill Book Co. Inc. (1955) 672.
21. J.B. Junt et al., Nucl. Instr. and Meths. 85 (1970) 269.
22. M.W. McNaughton et al., Nucl. Instr. and Meths. 116 (1974) 25.

23. R.A. Riddle et al., Nucl. Instr. and Meths. 121 (1974) 445.

24. D.G. Crabb and J.G. McEwen, Nucl. Instr. and Meths. 48 (1967) 87.

25. J.C. Young et al., Nucl. Instr. and Meths. 68 (1969) 333.

26. M. Drosg, Nucl. Instr. and Meths. 105 (1972) 573.

27. S.T. Thornton and J.R. Smith, Nucl. Instr. and Meths. 96 (1971) 551.

28. A.S. Parsons et al., Nucl. Instr. and Meths. 79 (1970) 43.

29. Servin Physical and Life Sciences, Geophysics and Industry, Nuclear Enterprise Ltd. (Catalogue 1970).

30. J.B. Birks, Phys. Rev. 84 (1951) 364.

31. J.E. Yurkon and A. Galonsky, Michigan State University, USUCL-295 (1979).